Feature-based Control of Visibility Error: A Multi-resolution Clustering Algorithm for Global Illumination

François Sillion[1]   *George Drettakis*[2]

[1]CNRS   [2]ERCIM-INRIA
*i*MAGIS
B.P. 53, 38041 Grenoble Cedex 9, France.

Abstract

In this paper we introduce a new approach to controlling error in hierarchical clustering algorithms for radiosity. The new method ensures that just enough work is done to meet the user's quality criteria. To this end the importance of traditionally ignored visibility error is identified, and the concept of *features* is introduced as a way to evaluate the quality of an image. A methodology to evaluate error based on features is presented, which leads to the development of a *multi-resolution visibility* algorithm. An algorithm to construct a suitable hierarchy for clustering and multi-resolution visibility is also proposed. Results of the implementation show that the multi-resolution approach has the potential of providing significant computational savings depending on the choice of feature size the user is interested in. They also illustrate the relevance of the feature-based error analysis. The proposed algorithms are well suited to the development of interactive lighting simulation systems since they allow more user control. Two additional mechanisms to control the quality of a simulation are presented: The evaluation of internal visibility in a cluster produces more accurate solutions for a given error bound; a progressive multi-gridding approach is introduced for hierarchical radiosity, allowing continuous refinement of a solution in an interactive session.

Keywords: Visibility error, Clustering, Feature-based error metric, Multi-resolution visibility, Hierarchical radiosity, Progressive multi-gridding, Global Illumination.

1 Introduction

Modern global illumination algorithms allow the precise simulation of interreflection effects, penumbrae caused by extended light sources, and subtle shading variations caused by complex reflectance properties [2, 15]. Lighting simulation systems operate under very tight and often contradictory constraints: users typically require guaranteed and easily controllable precision levels, with maximum speed for interactive design. An important goal of rendering research is thus to enable the user to reduce the solution error where such reduction is deemed desirable, while at the same time limiting the time spent to achieve this reduction.

Unfortunately, the algorithmic complexity of radiosity methods (quadratic in the number of objects) in effect impairs their use for scenes containing more than a few thousands objects, while Monte-Carlo methods are unable to provide low and medium-quality solutions without too much noise. Therefore means must be found to focus the effort on the most important parts of the calculation.

This paper presents new algorithms and criteria that together allow very fine and efficient user control of the perceived quality of a solution. This is accomplished by first acknowledging the importance of *visibility error*, and using the concept of *features* to evaluate the quality of a solution. This leads to the introduction of *multi-resolution visibility*, which allows precise control of the quality vs. time tradeoff. Additional mechanisms are then discussed to control the quality of a simulation in a working system.

Previous work: error-driven computation and visibility

The introduction of the hierarchical radiosity algorithm [5] was a major step towards the design of practical lighting simulation systems. First, it reduces the overall resource requirements for a given solution. Second, it uses a surface subdivision criterion as an explicit control mechanism. This criterion embodies the priorities used to guide the simulation, as it directs the computational effort to "areas of interest", introducing a natural tool for error estimation.

Hierarchical radiosity (HR) remains quadratic in the number of input objects (since each pair of objects must be linked before hierarchical subdivision begins), and therefore is not suited to large collections of small objects. *Clustering*, the operation of grouping objects together into composite objects that can interact, provides a means to eliminate the quadratic complexity term. Such clustering can be performed manually [11, 7] or automatically [16, 13].

Historically, subdivision criteria for HR first consisted of simple bounds on either the form factor or the exchange of radiosity between two surface patches [5], under the assumption that the error incurred is proportional to the magnitude of the transfer. Using the concept of importance these bounds can be made dependent on the user's interest for each region [17]. However such bounds tend to be quite conservative and thus produce unnecessary subdivision [6].

Recent work has attempted to characterize possible sources of error in global illumination [1], and establish error bounds on radiosity solutions [8]. These error bounds can then be used in the subdivision criterion of a hierarchical algorithm. Since the estimation of the error is decoupled from that of the actual transfer, subdivision can be avoided in regions where significant transfers take place without much error, resulting in better focus of the computational expense.

Existing error controls however typically ignore visibility as a possible source of error, or simply increase the error estimate by a constant factor in situations of partial visibility. Trivial bounds of 0 (total occlusion) and 1 (total visibility) are often used. While these

bounds are always valid, their use results in unnecessary work being done to narrow down other error bounds by increasing the subdivision. Global visibility algorithms can be used to exploit the structure of architectural scenes and produce guaranteed visibility information [18], but they are not suited to large collections of independent objects. For exchanges between surfaces, *discontinuity meshing* also provides explicit visibility information, and indeed considerably improves the efficiency of HR [10]. However for Monte-Carlo or clustering approaches it is either impossible or impractical to calculate analytic visibility and error bounds must be used. For exchanges between clusters, an approximate visibility estimate can be derived using equivalent volume extinction properties [13], but the error introduced in the process has not yet been analyzed.

Visibility error is admittedly difficult to evaluate, since the computation of visibility itself is a costly process. Still, controlling this source of error is imperative since the quality of shadows plays a significant role in determining the user's perception of image quality. In complex environments where clustering is most useful, a dominant part of computation time is spent in visibility calculations involving small, geometrically complex objects. Resulting visibility variations produce fine detail shadows, which may be of little interest to the user, or may be lost in the implicit averaging over a surface patch.

Paper overview

The preceding discussion has shown that a key issue in designing efficient lighting simulation systems is to provide adequate control mechanisms to ensure that just enough work is done to meet the user's quality criteria. It appears that control of visibility error has not yet been attempted, despite its great potential for tightening global bounds and reducing computation costs. The goal of this paper is twofold: first, a new approach to visibility error estimation is proposed, based on *features*, that legitimates the use of a *multi-resolution visibility* algorithm. Second, quality control mechanisms are discussed for interactive simulation systems development.

We begin in Section 2 with the introduction of features to evaluate image quality, and show why existing error metrics are incapable of determining when a given level of detail is satisfactorily represented. A simple metric is then proposed to illustrate how to take into account the user's interest in a minimal *feature size*. This leads to Section 3 where we explain how to compute *multi-resolution visibility* information using a spatial hierarchy augmented with equivalent *extinction* properties. Selection of a hierarchical level for visibility computation can then be based on the resulting feature size on the receiver. In this paper an application to clustering algorithms is discussed, but multi-resolution visibility is equally promising for Monte Carlo techniques. The construction of a suitable hierarchy is discussed in Section 4. In Section 5 we show that the multi-resolution visibility algorithm successfully generates images (currently for isotropic clusters) in which only selected features sizes are accurately represented, resulting in computational savings. Section 6 presents more quality controls for clustering algorithms, specifically intra-cluster visibility determination in linear time and progressive multi-gridding. We conclude in Section 7.

2 Feature-Based Error Analysis

To a large extent the quality of an image is judged based on how well features of different sizes are represented. It is not easy to characterize what constitutes an illumination feature. For the purposes of this paper, we will consider image features to be the connected regions of varying illumination related to shadows (regions in umbra or penumbra).

2.1 L^p metrics are inadequate for "feature detection"

A major difficulty for accurate lighting simulation is that in general the exact solution is not known at the time of computation. Thus the estimation of the error in a proposed approximation is particularly difficult, and must rely on the computation of error bounds for all algorithmic operations. Even in the case where an exact solution is available, it is not a simple task to define the quality of a given approximation. This is done by choosing a particular error metric to quantify the distance between an approximate solution and the true solution. A "good" metric should therefore convey a sense of the user's requirements. A central observation in this paper is that when simulating a complex scene, the user is typically interested in capturing illumination variations down to a certain scale. Very small details are not as important, or at least not in all areas of the scene. We strive to define a control mechanism that will avoid any work that would only generate such small details.
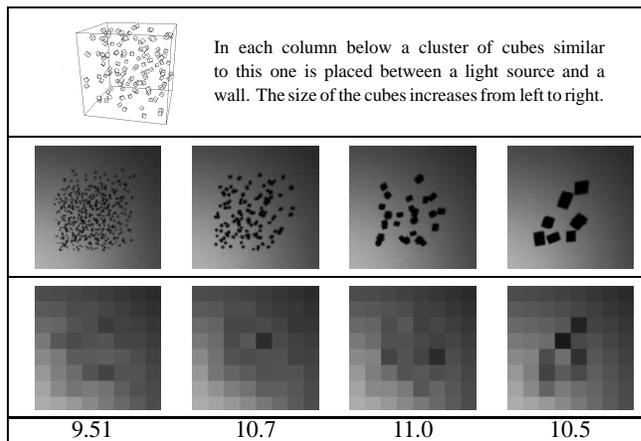

Figure 1: Comparison of approximate illumination solutions using different clusters. Top: reference images (illumination of the wall). Middle: approximate images using a coarse mesh. Bottom: L^2 error norms. Note that the four images have similar L^2 error values, and all hide some illumination information. However the varying size of the missing features cannot be discovered.

Figure 1 illustrates the issue by showing shadows cast on a wall by four different groups of objects. Four approximate images, all computed using the same mesh size, are shown below the "exact" images. Consider a user who is interested in shadows of a specific size, e.g. those of the image on the extreme right, but is satisfied by the averaging of the smaller, detailed shadows on the left[1]. The user thus does not wish more work to be done for the detail shadows, but wishes to have a more accurate representation at the larger scale. The subdivision criterion used in a HR algorithm for instance should be capable of halting the subdivision for the left-hand group, while ordering further computation for the group on the right. Thus an error measure should distinguish between the four cases.

Traditional error metrics are incapable of making such a distinction. As an example consider the commonly used family of error metrics expressing the distance between a reference function f and an approximate function $\widehat{f}$ as the L^p norm

$$\|\widehat{f} - f\|_p = \left(\int |\widehat{f}(x) - f(x)|^p dx \right)^{\frac{1}{p}}$$

---

[1]Perhaps a more realistic example would be a situation where a user is viewing an office scene from the doorway, and in which accurate shadows for chairs and desks are important, but averaged, low quality shadows from details such as pens on a desk are satisfactory.

L^p norms simply add error contributions from all points on a surface (or in an image), and do not take into account higher-level properties of the radiance distributions, such as the size and shape of illumination features. This is illustrated by the similar values obtained for the four groups in Figure 1. Appendix A shows that in fact for a point light source the L^1 or L^2 error introduced by averaging all visibility variations depends only on the average visibility, and not on the size or shape of the shadows.

2.2 A proposal for an error metric based on feature size

Our hypothesis is that illumination features (shadows or bright areas) are important only as far as they have a significant visual impact. Therefore it is possible to define a *feature size* on a receiving surface, and decide that features smaller than that size are "unimportant": their absence should not contribute to the error.

In the remainder of the paper we refer to the radiosity function over a surface as an "image". This terminology should not mask the important fact that the entire discussion takes place in three-dimensional object space. In order to demonstrate the relevance of the feature-based approach, we assume for now that we have access to all the information in a reference solution. The multi-resolution visibility technique of Section 3 will show how the ideas developed here can still be used in the absence of such a reference.

A simple error metric based on features is defined by segmenting the image f into two components by means of a *feature mask* $\mathcal{F}^s(f, x)$: a binary function that equals one at points x that belong to a "feature" (of size greater than s) of function f. Computation of feature masks from the reference solution is described in the next section. For points in the mask region we compute an L^p norm of the difference between the approximate function and the reference function. For points outside the feature mask, we are content with an average value (since features present there are smaller than s). Thus in our current implementation we compute average values at each point, for both the approximate and reference functions, using a box filter of size s around the point of interest, and compute an L^p norm of the difference between the averages.

The feature-based error metric (FBEM) is summarized by the following formula, where $\overline{f^s}$ represents the filtered version of f:

$$\|\widehat{f} - f\|_p^s = \left(\int |\overline{\widehat{f}^s}(x) - \overline{f^s}(x)|^p \left[1 - \mathcal{F}^s(f, x)\right] dx \right.$$
$$\left. + \int |\widehat{f}(x) - f(x)|^p \mathcal{F}^s(f, x) dx \right)^{\frac{1}{p}} \quad (1)$$

2.3 Examples

Table 1 shows the FBEM values computed for the four groups of Figure 1 and different values of the minimum feature size s. The object-space size of typical shadows in these images is respectively 11, 16.5, 22 and 31. For small s values, all FBEM values are high since the metric is equivalent to an L^2 metric in the limit of $s = 0$. As s increases, FBEM values decrease more rapidly for the groups containing smaller objects, as expected. There appears to be a residual error of about 3 due to the mesh size used for the approximate solutions.

Assume the user is interested in clearly seeing features of size 30 or greater, while being content with an average for all features smaller that this size. The extreme right-hand image of Figure 1 requires more work since the FBEM value for $s = 30$ is high. The approximation for the other three images is deemed satisfactory since the error is low.

Thus, using the FBEM presented above, it is possible to reveal the presence of features greater than a given threshold in the approx-

Feature size:				
5	14.76	16.34	17.25	17.31
16	9.37	12.24	15.76	15.80
24	4.78	6.50	9.06	14.74
30	4.23	3.16	6.90	13.37
40	3.65	2.33	3.35	6.94

Table 1: Feature-based error metric (FBEM) for the four approximate images of Figure 1 and five different feature sizes. The four measures are equivalent for small feature sizes, and decrease at different rates as a function of s. Images are shown again for clarity.

imate images, opening the way for selective subdivision based on the user's minimum feature size of interest. Of course this could not be used *as is* in a subdivision criterion for HR, since it uses a reference solution, but it is useful for *a posteriori* validation of control mechanisms.

2.4 Computation of feature masks

According to the definition of features given above, computing a feature mask amounts to identifying connected regions of "significant" size. Mathematical morphology provides tools to isolate features based on their size [12]. Consider a binary image, representing for example the characteristic function of an object. We define the action of an *Erosion* operator as follows: all points outside the object (white) are untouched. All points inside the object that have a neighbor outside become white. All other points remain black. An *Expansion* operator is defined similarly by including in the objects all outside points that have a neighbor in the object. Figure 2 shows a reference image and images obtained after a number of erosions (top) or expansions (middle).

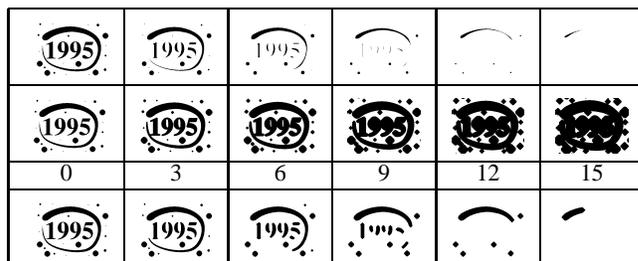|					
0	3	6	9	12	15

Figure 2: Effect of repeated applications of the erosion (top), expansion (middle) and combined erosions/expansion (bottom) operations on a binary image. The reference image appears in the left column, and the number of applications of the operators increases from left to right. For the bottom row we apply n erosions followed by n expansions.

Clearly an object of diameter $2d$ will disappear after d erosions are applied in sequence. Thus applying a sequence of n erosions followed by n expansions will successfully eliminate all small regions, but keep larger regions (slightly modifying their shape in the process). This process is illustrated in the bottom row of Figure 2.

Computing the effect of the erosion operator on a binary image is straightforward using bitwise operations: the result is the logical OR of the image and the four translated copies of itself (by one pixel) in the $+x$, $-x$, $+y$ and $-y$ directions. For the expansion operator the logical operator AND is used.

In our examples, the original binary image is computed by recording all areas of the receiver that have a partial or occluded

view of the light source. This expensive operation was performed only once during the creation of the reference image. Feature masks are computed by applying the proper number ($p/2$ for a feature size of p) of successive erosions and expansions to eliminate unwanted features. Figure 3 shows some feature masks for the four groups used above.

Original mask	F Size 12	F Size 18	F Size 24

Figure 3: Some feature masks for the images in Figure 1.

3 A Multi-resolution Visibility Algorithm

In the previous section we presented the concept of a *feature size* and introduced an error metric which permits the evaluation of image quality determined by how well illumination features are represented. We now use these fundamental concepts to develop a *multi-resolution* (MR) visibility algorithm. With this algorithm, expensive high quality visibility calculations are only performed when they are expected to help in the accurate representation of features deemed "interesting" by the user.

Hierarchical spatial subdivision structures are often used in the calculation of global illumination algorithms, in particular when form-factor estimation is performed with ray-tracing [19, 4, 5, etc.]. In radiosity clustering algorithms the hierarchy of clusters is also used for radiometric calculations, by letting clusters represent their contents for some energy transfers [13, 16]. The following *multi-resolution visibility* algorithm naturally extends previous clustering approaches by allowing clusters to also represent their contents in some visibility calculations. If a specific feature size s has been chosen, it is unnecessary to consider the contents of a cluster for visibility if these contents will produce features smaller than s.

3.1 Approximate visibility computation between clusters using an extinction model

Let us assume that we have grouped all objects in the scene into a hierarchy of clusters. Approximate visibility calculations can be performed using an analogy between clusters and absorbing volumes [13]. The approximation (asymptotically exact for homogeneous isotropic clusters when the size of the objects goes to zero) consists of associating an *extinction coefficient* κ with each cluster. The transmittance function between two points P and Q in the scene is

then given by

$$
\begin{aligned}
T(P,Q) &= e^{-\int_{PQ} \kappa(u)\,du} \\
&= e^{-\sum_{i\in\mathcal{C}(PQ)} \kappa_i l_i}
\end{aligned}
$$

where $\mathcal{C}(PQ)$ is the set of clusters traversed by the ray joining P and Q, κ_i is the extinction coefficient of cluster i, and l_i is the length traveled inside cluster i by the ray.

Extinction coefficients express the probability that a random ray is intercepted in the cluster, and are computed as

$$
\kappa_i = \frac{\sum_j A_j}{4V_i}
$$

where the area of all surface patches contained in cluster i is summed and divided by the cluster's volume. Since a surface contributes to the extinction of only one cluster, the attenuation due to overlapping clusters is correctly obtained by adding their extinction contributions.

3.2 Multi-Resolution Visibility

In the rest of this section we consider the emitter-blocker-receiver configuration shown in Figure 4, which consists of two surfaces, the emitter E and the receiver R, in two-dimensions. This restriction is for presentation purposes only and is removed later.
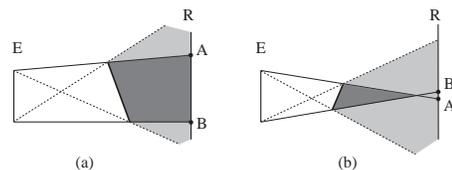

Figure 4: Definition of shadow features created by a blocker. (a) The umbra region is unbounded since the blocker is larger than the emitter: there is always an umbral region on the receiver. (b) For some positions of the blocker the receiver has no umbral region.

If a blocker (which for now we also consider to be a surface) is placed between the emitter and the receiver, *umbra* and *penumbra* regions are created in space. Depending on the position of the blocker, there may or may not be an umbral region on the receiver. (Figure 4). Given the definition discussed above the size of the umbral zone on the receiver $-AB$ in Figure 4(a)–, if it exists, is the *feature size*.

The blocker may actually be a hierarchical representation of a collection of objects (a *cluster*) as pictured in Figure 5(a). In this case, at each level of the hierarchy an extinction coefficient is stored allowing the approximate calculation of the attenuation of a ray if it passes through the cluster, as described previously.

Multi-resolution visibility can be performed by avoiding the descent into the hierarchy after a certain level. When the required conditions are met the extinction coefficient is used instead, thus avoiding the intersection of the ray with all the descendants of this cluster. Evidently, the effect is that visibility is no longer exact, but an average estimation of transmittance. It is here that a large potential gain in computation time can be achieved. In scenes where the small detail objects (e.g., models of phones, keyboards, small objects on a desk etc.), comprise the largest part of the geometric complexity, the intersection with these objects can quickly become the overwhelming expense of visibility (and overall) computation. By considering

the higher level clusters for visibility computation instead of the numerous contents, when such a choice is dictated by the chosen feature size, this expense can be completely avoided.
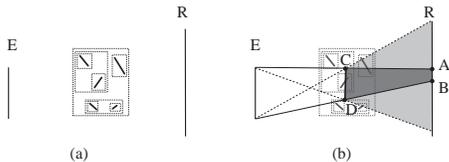

Figure 5: Visibility estimation through a cluster. (a) the blocker is a hierarchy of clusters. (b) an "equivalent blocker" is used to estimate the maximum feature size on the receiver.

Recall the discussion in Section 2 in which the user wishes to accurately represent all features of size greater than s on the receiver. To achieve this, all that is required is to descend sufficiently far into the hierarchy so that the large shadows are accurately calculated, while performing the approximate calculation for small, detail shadows.

To facilitate such a choice each cluster is augmented with a description of the maximum blocker size *BSIZE* of its contents (we give a precise definition of this in the following section). It then suffices to place a fictitious blocker of size *BSIZE*, at the center of the actual cluster $-CD$ in Figure 5(b). The descent in the cluster hierarchy can be terminated if the projected umbral region of the fictitious blocker (AB in Figure 5) is smaller than the chosen feature size s.

Contiguous regions which let light traverse must also be considered as feature creators since a feature can be considered "negative" (umbra in a bright region), or "positive" (lit areas inside a dark region). We thus extend our definition of features from Section 2 by defining *BSIZE* to be the maximum of the connected regions of light or shadow. This is consistent with the symmetric expression of visibility error with respect to umbra and light presented in Appendix A.

3.3 Characterization of a Cluster for MR Visibility

All that is required in order to apply the preceding algorithm is the determination of *BSIZE* for each cluster. The restriction to two-dimensions is now lifted, and the treatment for three-dimensional clusters is described. For now clusters are assumed to contain objects placed so that the cluster density can be considered isotropic, and thus does not depend on the direction of incidence of a ray.

The goal is to determine a representative size for a blocking cluster, which will allow the calculation of the maximum feature size given a specific emitter-receiver configuration. At first glance it may seem natural to take *BSIZE* to be the size of the largest object contained in the cluster. However there is one important consideration: it is the *connected region* of shadow on the receiver which we wish to consider. Furthermore, as discussed above, the regions of light potentially blocked by the contents of the cluster *and* the regions of light which pass through must be considered separately.

A preprocessing step is performed to calculate *BSIZE* for all clusters in the hierarchy. For each cluster, all the contained objects are orthographically projected into a binary image. This operation is performed for a given cluster and a given direction, resulting in a *view-independent* characterization. The consequence of the isotropic cluster assumption is that a single orthographic projection is sufficient. For non-isotropic clusters the *BSIZE* parameter is a function of the direction of interest. A simple solution in that case would be to interpolate from a number of sampled directions. Our current research focuses on more efficient representations for such directional information [14].

The erosion and expansion operators from Section 2.4 are then used to compute the maximum sizes for blockers and free regions inside a cluster. Erosions (respectively expansions) are computed until all objects have disappeared (respectively until all free space has disappeared). The *number* of erosion or expansion operations defines the value of *BSIZE* for the blocked and free regions respectively. In our implementation we do the projections, erosions and expansions using Graphics hardware.

4 A Hierarchical Structure for Clustering and Multi-Resolution Visibility

Previous automatic clustering approaches have used spatial data structures developed for ray-tracing (hierarchical bounding boxes [3] were used in [16], while in [13] a K-D tree was used). In this section we show that given the calculation of average visibility based on extinction coefficients in the manner of [13], it is beneficial to develop a special-purpose hierarchical data structure, such that the resulting clusters have properties suitable for cluster-based hierarchical radiosity and multi-resolution visibility.

By definition, clusters are constructed to *represent* as accurately as possible the collection of objects they contain. By introducing computation of visibility using extinction coefficients and also multi-resolution visibility, apart from the representation of energy transfer of the contained objects as a whole, the clusters also need to correctly represent the transmission properties of the collection of contained objects.

These two modes of representation place different constraints on the cluster hierarchy. From the point of view of energy exchanges, good clusters allow tight bracketing of radiance or visibility functions (thus surfaces with similar orientation that do not shadow each other are preferred). From the point of view of visibility approximation, good clusters are ones for which the extinction property is plausible (thus homogeneous isotropic clusters are preferred). Given these constraints, we have identified two key properties for clusters: (a) *proximity* and (b) *homogeneity* of the contained objects. Maintaining proximity is a natural way to group objects when the cluster is used to represent radiative transfers. Also, for multi-resolution computation it is important that objects contained in a cluster are close so that the averaging performed does not introduce unacceptable artifacts. Homogeneity here means that we want a cluster to group objects of similar size, and is crucial for the resulting quality of the average visibility computation.

As a simple measure of proximity, we use the percentage of empty space resulting from a clustering operation (i.e., the addition of an object or a cluster to another cluster). Thus we prefer clusters in which the empty space is minimized.

To efficiently group objects of similar size we use a hierarchy of n levels of uniform grids. We start with level 0, which is a single voxel the size of the bounding box of the scene and then at each level i we create a grid which is subdivided into 2^i voxels along each axis. We then insert each object into the level for which its bounding box fits the voxel size.

Once these grids have been constructed, we start at the lowest level n, containing the smallest objects. We group the objects entirely contained in each voxel, by attempting to minimize the empty space, in accordance to the proximity criterion described above. In addition, objects which are very small compared to the grid size are grouped into an appropriate cluster, even if the resulting cluster is largely empty. Once all the voxels of a level have been treated, we attempt to add the objects not entirely contained in a single voxel at this level to the clusters already constructed, again using the same criteria. We then insert the clusters created to the grid of the level immediately above, and iterate.

Once the cluster hierarchy has been created, the data structure is augmented with average transmission behavior by propagating the average extinction values up the hierarchical structure as in [13].

When multi-resolution visibility is used, the $BSIZE$ estimation is also performed for each cluster in the hierarchy in the manner described in Section 3.

Figure 6 presents results obtained with the new hierarchy using first a surface visibility algorithm similar to that of [16], and then the average visibility proposed in [13]. The scene consists of 5380 polygons. It is interesting to observe the significant time gain achievable by the average visibility algorithm given a suitable hierarchy (we observe a factor of 4), while approximate shadows are preserved.

| Surface vis: 1 216 s. | Volume vis: 376 s. |

Figure 6: Timings (in seconds) using the new hierarchy construction. Throughout the paper all timing information was obtained on an Indigo R4000 computer.

Constructing a suitable hierarchy for cluster-based hierarchical radiosity with extinction and multi-resolution visibility is a difficult problem. The results indicate that the first solution presented here, based on proximity and homogeneity, results in the construction of hierarchies well suited to approximate and multi-resolution visibility calculations.

5 Results of multi-resolution visibility

We have implemented the hierarchy construction, the calculation of *BSIZE* and the multi-resolution visibility algorithm in a hierarchical radiosity clustering testbed.

To evaluate the results of the multi-resolution visibility approach we have computed images of test environments using different values for the feature sizes of interest s on a receiver.

The first test scene is shown in Figure 7 (left). It contains the four clusters used in Section 2 and a light source (in yellow). The right-hand image is the illumination obtained on the back wall and serves as a reference image. For all these images visibility was always computed solely using extinction properties (thus we do not attempt to characterize the error introduced by averaged transmission visibility itself).

Figure 8 shows four images, where the desired feature size parameter (see Section 2.2) is changed. For each image the computation time in seconds is given. A very low error threshold was used to ensure that the mesh density was maximal for all images. Thus the decrease in computation time as the desired feature size becomes larger measures the speedup in the visibility calculation.

We next show that multi-resolution visibility is consistent with the feature-based error metric (FBEM) from Section 2.2, by computing the FBEM for the images described above. Although the four clusters have been grouped in a single image for simplicity, we apply the error metric only on the region of the image corresponding to each cluster, to obtain an FBEM value for each of the four groups.

For the four images, we show for each cluster the value of L^2 error norm (back row) and the value of the FBEM for a feature size s equal to that used in the MR Visibility algorithm. We note that
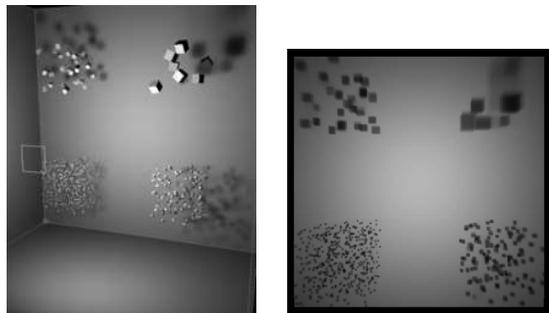
| 3D view of test scene. | Reference sol. (2069 s). |

Figure 7: Reference image used in the error comparisons.

as we increase s the L^2 norm for all clusters increases, as more and more averaging is being performed. Still the increase appears later for larger objects, as expected. The FBEM values are always of similar magnitude, despite the fact that very different levels of averaging are being used in different clusters in a given image. This shows that the multi-resolution visibility algorithm accomplishes its purpose: given a desired feature size, it ensures that the corresponding FBEM remains low while allowing time gains.

Figure 9 shows that even greater speedups can be achieved when a medium error threshold allows MR visibility to reduce the amount of subdivision. The explicit incorporation of MR visibility in refinement criteria is a promising path for further acceleration.

6 Control of Image Quality for Clustering

Recent algorithms separate the computation of high-quality images into two phases: a coarse quality global illumination calculation is first performed using elaborate algorithms such as discontinuity meshing or clustering in a *global pass*. A view-dependent, potentially very expensive *local pass* follows [9, 16]. This local pass is typically a ray-casting operation: at each pixel the energy from all the links is collected, allowing the calculation of high-quality shadows. The cost of this local pass is often many times larger than that of the light-transfer calculation using clusters. In essence this pass may eradicate all computation time benefit achieved by using the clusters in the first place, and exclude any possibility for interactivity with quality and error control.

In contrast, we maintain a "progressive refinement" philosophy, by providing explicit quality controls, allowing computational cost to be focused on desired characteristics of the resulting image. The first component of this approach is the multi-resolution visibility presented above. This technique, coupled with the use of *importance* [17] to assign appropriate feature sizes to different objects could plausibly replace the global/local pass approach while affording more interactivity. We present next two supplementary quality controls: first, the correct treatment of intra-cluster visibility and second, progressive multi-gridding permitting rapid interactive response for hierarchical radiosity.

6.1 Intra-cluster visibility

Previous clustering algorithms compute a bound on energy transfer that ignores visibility (bound of 1 on the visibility error), both between the two clusters but also in the distribution of light on each side [16, 13]. This potentially results in light leaks at the scale of the cluster. This behavior is not only visually displeasing but also flawed: since bounds are computed on irradiance values, that irradiance is distributed to many surfaces which should be shadowed,

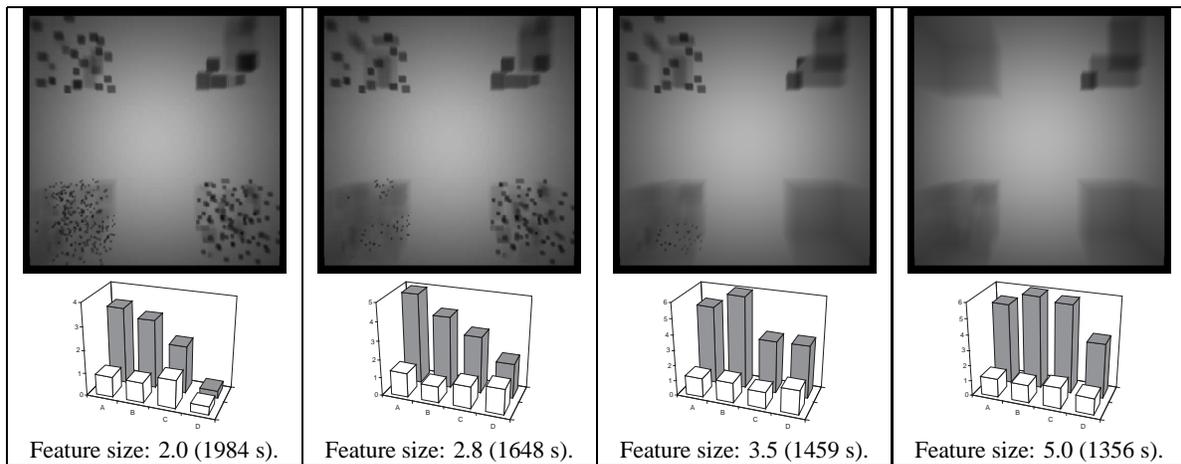| Feature size: 2.0 (1984 s). | Feature size: 2.8 (1648 s). | Feature size: 3.5 (1459 s). | Feature size: 5.0 (1356 s). |

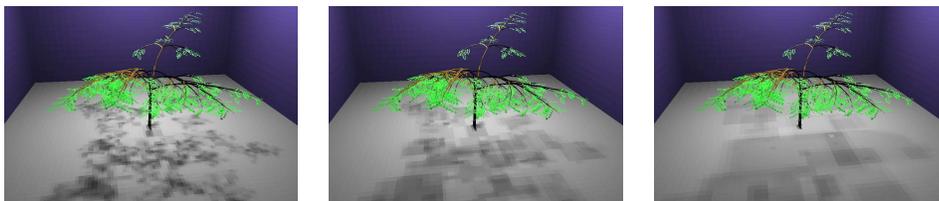Figure 8: Results for the multiresolution visibility algorithm.

Figure 9: Increasing the desired feature size reduces both the amount of subdivision and the cost of visibility computations. (left) Fsize = 0, $621s$. (middle) Fsize = 4, $245s$. (right) Fsize = 8, $148s$. Tree courtesy of CIRAD, modelled with 7967 polygons using AMAP.

thereby creating energy.

If visibility information inside the cluster with respect to a source cluster can be computed (with some approximation) in time linear in the number of contained objects, the overall time and space complexity of $O(s \log s)$ for clustering is not modified [16].

We propose the use of an item buffer to quickly evaluate this visibility. The cluster's contents are projected in the direction of the light source using a z-buffer to determine visible surfaces from that direction. By counting instances of an item number in the buffer we obtain an estimate of the projected area of each patch visible from the direction of the source. This is used as the projected area in kernel calculations when computing energy bounds. Note that the resolution of the item-buffer can be adapted to the contents of each cluster, provided we know the size of the smallest object in each cluster. Thus the aliasing problems inherent to the item-buffer approach can be reduced. The same technique is also used at the other end of a link, to evaluate the energy leaving a cluster.
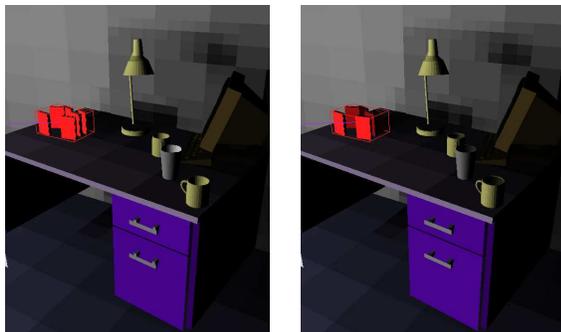

Figure 10: Results of introducing intra-cluster visibility.

In the images of Figure 10 we present an example where a link (shown in purple) has been created from the light source to a cluster of books. Ignoring intra-cluster visibility (left) results in the creation of energy since all books are fully illuminated. Using the vis-

ibility buffer to modulate the energy distribution (right), energy is preserved while improving the appearance of the image.

6.2 Progressive multi-gridding

In hierarchical radiosity algorithms subdivision is controlled by an error threshold on individual interactions. A global bound on error is difficult to determine and it is consequently difficult for the user to choose an error threshold so as to achieve a certain quality. The problem is exacerbated with clustering, since the subdivision of links is amortized with time, and thus successive iterations may become much more expensive as the allowed error decreases. This sharp and unpredictable increase in iteration time may then destroy interactivity.

As a remedy we develop a *progressive multi-gridding* approach. By analyzing the distribution of error bounds on the links created, we can predict how many of these links would survive a given decrease in the error threshold, and thus estimate the time required for a subsequent iteration with the new error threshold. In a manner more intuitive to the user the amount of computation can be specified (in the form of a maximum number of links to refine) and the system proceeds to deduce the new threshold to use for hierarchical refinement.

This analysis can be performed at a marginal cost by recording a histogram of the distribution of error bounds computed. Specifically, the interval between 0 and the current error threshold ε is divided into a number of bins, each associated with a counter. Every time a link is created (or left unchanged) during the hierarchical subdivision procedure, we increment the counter for the bin corresponding to the link's error bound. At the start of the next progressive multi-gridding iteration, the new error threshold is chosen such that the sum of all counter for bins with higher error levels is less than a user-specified limit k. This effectively chooses an error threshold such that at most k links are refined. This multi-gridding algorithm does not accelerate the computation but guarantees a continuous update of the simulation.

7 Conclusions

Important advances towards the goal of providing interactive systems capable of treating very complex environments have been made by hierarchical radiosity and clustering algorithms. Nonetheless several important shortcomings of previous approaches were identified in this paper: (a) visibility error is typically ignored, (b) traditional error metrics do not allow the user to specify a desired level of detail and (c) progressive refinement of the simulation is difficult to achieve.

In this paper we introduced a new approach to error estimation based on illumination *features*, which allows the user to choose a level of detail relevant to a given simulation. The quality of a solution then relates to how well features of the user-determined size have been represented.

The principles introduced by the feature-based analysis were used to develop a *multi-resolution visibility algorithm*. The hierarchy constructed for clustering contains transmission information as in [13] and is further augmented with an estimate of the largest equivalent blocker size from its contents. This information is used to limit the cost of visibility calculations. An algorithm which efficiently constructs a suitable hierarchy was also presented. The results of the implementation for isotropic environments show significant computational speedup using MR visibility when the user does not require the accurate representation of small features.

Two additional quality control mechanisms were introduced: *intra-cluster visibility* which corrects potential light-transfer error suffered by previous clustering algorithms, and *progressive multigridding* which is essential for interactive clustering systems.

We believe that the introduction of feature-based error and quality evaluation is an important step which will lead to significant acceleration of global illumination algorithms. Multi-resolution visibility is an example of such an achievement.

In future work the extension of our approach to non-isotropic environments must be completely developed. Promising first results in representing directional information for clustering have been obtained [14]. We have not yet addressed the analysis of error caused by the use of extinction coefficients and the effect of visibility correlations between clusters and their contents. Research in these areas is extremely important for the development of reliable quality controls. It will be interesting to observe the results of the application of our approach to Monte Carlo methods. A more in-depth study of feature-based error metrics must be performed. Finally better algorithms for hierarchy construction should be investigated.

8 Acknowledgements

References

[1] James Arvo, Kenneth Torrance, and Brian Smits. A framework for the analysis of error in global illumination algorithms. In *Computer Graphics Proceedings, Annual Conference Series:* SIGGRAPH '94 (Orlando, FL), pages 75–84, 1994.

[2] Michael F. Cohen and John R. Wallace. *Radiosity and Realistic Image Synthesis*. Academic Press, Boston, 1993.

[3] J. Goldsmith and J. Salmon. Automatic creation of object hierarchies for ray tracing. *IEEE Computer Graphics and Applications*, 7(5):14–20, May 1987.

[4] Eric A. Haines. Shaft culling for efficient ray-traced radiosity. In P. Brunet and F.W. Jansen, editors, *Photorealistic Rendering in Computer Graphics*, pages 122–138. Springer Verlag, 1993. Proceedings of the Second Eurographics Workshop on Rendering (Barcelona, Spain, May 1991).

[5] Pat Hanrahan, David Saltzman, and Larry Aupperle. A rapid hierarchical radiosity algorithm. *Computer Graphics*, 25(4):197–206, August 1991. Proceedings SIGGRAPH '91 in Las Vegas.

[6] Nicolas Holzschuch, François Sillion, and George Drettakis. An efficient progressive refinement strategy for hierarchical radiosity. In *Fifth Eurographics Workshop on Rendering*, Darmstadt, Germany, June 1994.

[7] Arjan J. F. Kok. Grouping of patches in progressive radiosity. In *Proceedings of Fourth Eurographics Workshop on Rendering*, pages 221–231. Eurographics, June 1993. Technical Report EG 93 RW.

[8] Dani Lischinski, Brian Smits, and Donald P. Greenberg. Bounds and error estimates for radiosity. In *Computer Graphics Proceedings, Annual Conference Series:* SIGGRAPH '94 (Orlando, FL), pages 67–74, July 1994.

[9] Dani Lischinski, Filippo Tampieri, and Donald P. Greenberg. Discontinuity meshing for accurate radiosity. *IEEE Computer Graphics and Applications*, 12(6):25–39, November 1992.

[10] Dani Lischinski, Filippo Tampieri, and Donald P. Greenberg. Combining hierarchical radiosity and discontinuity meshing. In *Computer Graphics Proceedings, Annual Conference Series:* SIGGRAPH '93 (Anaheim, CA), pages 199–208, August 1993.

[11] Holly Rushmeier, Charles Patterson, and Aravindan Veerasamy. Geometric simplification for indirect illumination calculations. In *Proceedings Graphics Interface '93*. Morgan Kaufmann, 1993.

[12] J. Serra. *Image analysis and mathematical morphology : 1*. Academic Press, London, 1982.

[13] François Sillion. A unified hierarchical algorithm for global illumination with scattering volumes and object clusters. *to appear in IEEE Transactions on Visualization and Computer Graphics*, 1(3), September 1995. (a preliminary version appeared in the fifth Eurographics workshop on rendering, Darmstadt, Germany, June 1994).

[14] François Sillion, George Drettakis, and Cyril Soler. A clustering algorithm for radiance calculation in general environments. In *Sixth Eurographics Workshop on Rendering*, Dublin, Ireland, June 1995.

[15] François Sillion and Claude Puech. *Radiosity and Global Illumination*. Morgan Kaufmann publishers, San Francisco, 1994.

[16] Brian Smits, James Arvo, and Donald P. Greenberg. A clustering algorithm for radiosity in complex environments. In *Computer Graphics Proceedings, Annual Conference Series:* SIGGRAPH '94 (Orlando, FL), pages 435–442, July 1994.

[17] Brian E. Smits, James R. Arvo, and David H. Salesin. An importance-driven radiosity algorithm. *Computer Graphics*, 26(4):273–282, July 1992. Proceedings of SIGGRAPH '92 in Chicago.

[18] Seth J. Teller and Patrick M. Hanrahan. Global visibility algorithms for illumination computations. In *Computer Graphics Proceedings, Annual Conference Series:* SIGGRAPH '93 (Anaheim, CA), pages 239–246, August 1993.

[19] John R. Wallace, Kells A. Elmquist, and Eric A. Haines. A ray tracing algorithm for progressive radiosity. *Computer Graphics*, 23(3):315–324, July 1989. Proceedings SIGGRAPH '89 in Boston.

A Visibility error using L^1 and L^2 norms

Consider a patch P illuminated by a point source at point y. To quantify the visibility error on the receiver patch, we compute the L^1 and L^2 norms of the difference between the visibility function $v(x, y)$ defined for $x \in P$, and its average value $\bar{v}$ over patch P. If P^+ is the region of patch P that receives light, $\bar{v}$ is equal to the ratio of the areas of P^+ and P. Separating the integrals into one over P^+ and one over $(P - P^+)$, we find

$$\|v - \bar{v}\|_1 = 2\bar{v}(1 - \bar{v}) \tag{2}$$

and similarly for the L^2 norm

$$\|v - \bar{v}\|_2 = \sqrt{\bar{v}(1 - \bar{v})} \tag{3}$$

Note that both estimates only depend on the average visibility across patch P, not on the distribution of the visibility function. Also note the dependency in $\bar{v}(1 - \bar{v})$, yielding a small error for either almost complete occlusion or almost complete visibility.